DETERMINATION OF THE ACCURATE VALUES OF THE RATE CONSTANT AND THERMODYNAMIC PARAMETERS FOR THE ROTATION ABOUT THE C(sp^2)–C(aryl) BOND. 3-SUBSTITUTED *N*,*N*,2,4,6-PENTAMETHYLBENZAMIDES

Eva PŘIBYLOVÁ[1] and Miroslav HOLÍK[2,*]

Department of Theoretical and Physical Chemistry, Faculty of Science, Masaryk University, 611 37 Brno, Czech Republic; e-mail: [1] evap@chemi.muni.cz, [2] holik@chemi.muni.cz

Received September 28, 1998
Accepted November 15, 1998

Three programs for the ^{1}H NMR line shape analysis of systems with unequally populated sites have been tested in order to get highly accurate rate constants of the hindered rotation about a single bond using four published criteria. The programs differ in the number of optimized parameters. As test compounds, 3-(adamantan-1-carbonyl)-*N*,*N*,2,4,6-pentamethylbenzamide (**1**) and 3-(2-dimethylpropanoyl)-*N*,*N*,2,4,6-pentamethylbenzamide (**2**) were prepared. It was found that a supermodified simplex method with only six parameters optimized in one step gives the most accurate values of the rate constants. Consequently, the calculated thermodynamic parameters E_a, $\Delta H^{\neq}$ and $\Delta S^{\neq}$ lie in relatively narrow confidence intervals.

Key words: Rate constants; Thermodynamic parameters; NMR line shape analysis; Dynamic NMR spectroscopy; Axial chirality; Hindered rotation.

Sterically hindered ortho-disubstituted benzoyl derivatives are non-planar in their ground state with carbonyl group twisted from the molecular plane. When the benzene ring is unsymmetrically substituted by two acyl groups, then the molecule exists in two steric isomers which can be assigned to *Z* and *E* configurational isomers and represented by the following structures.

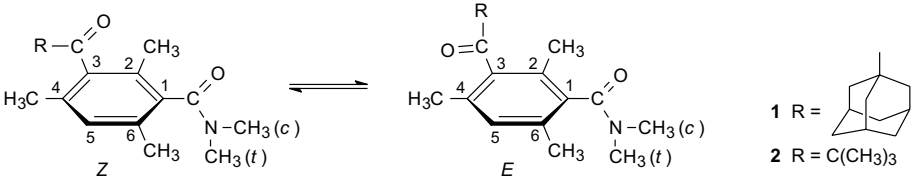

Obviously, the *E*–*Z* isomerization can proceed through the rotation about C1–CO bond (amide group rotation) or C3–CO bond (keto group rotation). We suppose that the latter takes place since the energy barriers at 390 K in model compounds 3-bromo-2,4,6-trimethylphenyl *tert*-butyl ketone[1] (89.7 kJ mol^{-1}) and 1-adamantyl 3-bromo-2,4,6-trimethylphenyl ketone[2] (93.4 kJ mol^{-1}) were found lower than that one for 3-bromo-*N*,*N*,2,4,6-pentamethylbenzamide[3] (106.1 kJ mol^{-1}). Approach to transition state by keto group rotation is about 150 and 50 times, respectively, more probable than that one due to amide group rotation. Similar results we obtained from the preliminary quantum-chemical calculations of compound **1**.

Application of dynamic ^{1}H NMR spectroscopy has proved to be a powerful tool for the study of such isomers[4–6]. If the steric hindrance in the planar transition state is sufficiently high, the rate of their interconversion can be investigated by ^{1}H NMR line shape analysis. The chemical shift difference of the signals of exchanging nuclei in two rotamers can be increased by addition a shift reagent in low concentration[4–6].

In the previous publication[1] from this laboratory, we demonstrated the suitability of Simtex program based on the supermodified simplex algorithm for the determination of accurate values of the rate constant and, consequently, of thermodynamic parameters. In that case, intramolecular motion in a form of exchange between two equally populated sites was monitored using a pair of signals.

The present work concerns the study of a system where an exchange between two unequally populated sites takes place. In order to obtain more accurate values of the rate constant, two amides, **1** and **2**, which make it possible to analyze line shape of the signals under coalescence of two independent pairs of signals, were studied. As regards the Simtex program, described in our previous paper[2], the line shape analysis of four singlets requires optimizing ten spectral parameters (four chemical shifts, four line widths, rate constant and isomer population), which could cause problems in finding the minimum of objective function during an optimization procedure. Therefore, two other programs, Simbex and Simseb, based on supermodified simplex algorithm and including a different number of optimized spectral parameters were tested.

In order to find out a reliable and precise optimization program for the line shape analysis, we have determined the rate constant of the rotation about the C(sp^1)–C(aryl) single bond in 3-(2-dimethylpropanoyl)-*N*,*N*,2,4,6-pentamethylbenzamide (**2**) using the above-mentioned programs written in our laboratory. Afterwards, the best program was used for determination of the rate constant of interconversion in a structurally related compound,

3-(adamantan-1-carbonyl)-*N*,*N*,2,4,6-pentamethylbenzamide (**1**), and the results for both studied amides were compared.

EXPERIMENTAL

Chemicals

All chemicals used, including the shift reagent tris(1,1,1,2,2,3,3-heptafluoro-7,7-dimethyl-4,6-octadionato)europium(III), $Eu(fod)_3$, were from Merck AG, Darmstadt, Germany. Synhydrid® was from Chemapol trade group, Czech Republic.

Synthesis

3-(Adamantan-1-carbonyl)-N,N,2,4,6-pentamethylbenzamide (**1**). Magnesium turnings (0.45 g, 0.019 mol) in a two-necked flask fitted with a reflux condenser with a calcium chloride tube and a dropping funnel, with an internal magnetic stirrer inside, were covered with tetrahydrofuran (9 cm^3) freshly distilled from sodium dihydridobis(2-methoxyethoxo)-aluminate (SDMA) (Synhydrid®). While heating the mixture under reflux, the reaction was started with ethyl bromide (0.2 cm^3) in 0.5 cm^3 of a solution of 1-adamantyl 3-bromo-2,4,6-trimethylphenyl ketone[1] (4.35 g, 0.012 mol), in tetrahydrofuran (31 cm^3). Then the rest of solution was added dropwise to the stirred mixture over a period of 50 min. After completing the addition, the mixture was refluxed until the magnesium turnings were dissolved (2.5 h). The Grignard reagent was poured onto solid carbon dioxide (100 g, 2.27 mol) and after its evaporation, the reaction mixture was decomposed by pouring into a mixture of concentrated hydrochloric acid (7.5 cm^3) and crushed ice (about 60 g). The organic layer was separated and the aqueous layer was extracted three times with 25-cm^3 portions of ether. The combined organic layers were dried with Na_2SO_4 overnight and the solvents were evaporated under reduced pressure. The crude acid crystallized from heptane (4 cm^3) in a refrigerator. Further purification involved dissolving acid in ether (20 cm^3) and extraction into 10% cold aqueous NaOH solution (10 cm^3). After separation, the aqueous layer was acidified with 20% HCl (5 cm^3) and the white crystals (0.78 g, 19.9%) of 3-(adamantan-1-carbonyl)-2,4,6-trimethylbenzoic acid were dried. This compound (0.78 g, 0.19 mol) was covered with thionyl chloride (15 cm^3) in a flask fitted with a reflux condenser and calcium chloride tube and refluxed for 2.5 h. An excess of thionyl chloride was co-evaporated with two portions of benzene (5 cm^3). After introducing dimethylamine gas into a solution of the acid chloride in ether (25 cm^3) for 5 min, the precipitate formed was filtered off and the product in solution left to crystallize for 3 days. Crystals were dissolved in chloroform (25 cm^3) and washed with water (2 × 15 cm^3); the organic layer was dried with Na_2SO_4 overnight and then the solvent was evaporated under reduced pressure. Amide **1** was obtained in a yield of 0.603 g (71%), m.p. 191–192 °C. ^{1}H NMR (500 MHz, $CDCl_3$, TMS, 305 K): 1.67 m, 6 H (Ad(γ)); 1.86 m, 6 H (Ad(α)); 1.97 m, 3 H (Ad(β)); 2.03 s, 3 H (2-Me); 2.15 s, 3 H (4-Me); 2.14 s, 3 H (6-Me); 6.84 s, 1 H (5-H); 3.11 s, 3 H (N–Me(*Z*,*cis*)); 3.10 s, 3 H (N–Me(*E*,*cis*)); 2.81 s, 3 H (N–Me(*Z*,*trans*)); 2.71 s, 3 H (N–Me(*E*,*trans*)). ^{13}C NMR (125 MHz, $CDCl_3$, TMS, 305 K): 17.7 s, 1 C (2-Me); 18.7 s, 1 C (4-Me); 20.5 s, 1 C (6-Me); 28.1 s, 3 C (Ad(β)); 36.4 s, 3 C (Ad(γ)); 39.1 s, 3 C (Ad(α)); 47.3 s, 1 C (C–CO); 140.2 s, 1 C (C-3); 135.0 s, 1 C (C-4); 133.2 s, 1 C (C-6); 132.6 s, 1 C (C-1); 129.4 s, 1 C (C-5); 128.2 s, 1 C (C-2); 218.3 s, 1 C

(CO); 170.9 s, 1 C (N-CO); 34.2 s, 1 C (N–Me(*cis*)); 37.4 s, 1 C (N–Me(*trans*)). For $C_{23}H_{31}N_2O$ (326.4) calculated: 78.15% C, 8.84% H, 3.96% N; found: 78.94% C, 9.24% H, 3.66% N.

3-(2-Dimethylpropanoyl)-N,N,2,4,6-pentamethylbenzamide (**2**). Amide **2** was synthesized by the same procedure as for **1** from 3-bromo-2,4,6-trimethylphenyl *tert*-butyl ketone[1,7]. The yield was 2.695 g (81%), m.p. 156–157 °C. ^{1}H NMR (500 MHz, $CDCl_3$, TMS, 305 K): 2.06 s, 3 H (2-Me); 2.19 s, 3 H (4-Me); 2.17 s, 3 H (6-Me); 6.88 s, 1 H (5-H); 3.14 s, 3 H (N–Me(*Z*,*cis*)); 3.13 s, 3 H (N–Me(*E*,*cis*)); 2.82 s, 3 H (N–Me(*Z*,*trans*)); 2.74 s, 3 H (N–Me(*E*,*trans*)); 1.22 s, 9 H (Me_3C). ^{13}C NMR (125 MHz, $CDCl_3$, TMS, 305 K): 17.4 s, 1 C (2-Me); 18.7 s, 1 C (4-Me); 20.2 s, 1 C (6-Me); 45.0 s, 1 C (**C**–CO); 140.6 s, 1 C (C-3); 135.0 s, 1 C (C-4); 133.2 s, 1 C (C-6); 132.4 s, 1 C (C-1); 129.5 s, 1 C (C-5); 128.0 s, 1 C (C-2); 219.1 s, 1 C (C–**C**O); 170.8 s, 1 C (N–**C**O); 34.2 s, 1 C (N–Me(*cis*)); 37.4 s, 1 C (N–Me(*trans*)); 28.1 s, 3 C (($\mathbf{C}H_3)_3$C). For $C_{17}H_{25}NO_2$ (275.4) calculated: 74.15% C, 9.15% H, 5.09% N; found: 74.15% C, 9.76% H, 4.90% N.

The assignment of ^{1}H and ^{13}C signals for amide **1** was checked by 2D heterocorrelated NMR spectrum HSQC and HMBC. The assignments of ^{1}H and ^{13}C signals for both compounds are in a good agreement with the corresponding signals of similar compounds, 3-bromo-2,4,6-trimethylphenyl *tert*-butyl ketone[1] and 1-adamantyl 3-bromo-2,4,6-trimethylphenyl ketone[2]. The *N*-methyl signals in **1** and **2** were assigned to *cis* and *trans* methyl groups by analogy to *N*,*N*,2,4,6-pentamethylbenzamide[4]; due to the twist of the amide group from the benzene plane, the methyl group *trans* to carbonyl approaches the shielding zone of the aromatic ring and its signal is shifted more upfield then that one of the *cis* methyl group. Assignment of signals to *E* and *Z* isomers was made by analogy to non-enolizeable β-oxo derivatives where quantum-chemical calculations[8,9] and NMR experiments[10,11] show that conformation with carbonyl groups oriented in the same direction, *i.e.*, *s-trans–s-trans*, is less probable than *s-cis–s-trans*. A dipol–dipol interaction model[12] also favours *E* configuration where the C=O dipoles are most nearly antiparallel over *Z* isomer with nearly parallel C=O dipoles. Therefore, the signals of lower intensity were assigned to *Z* isomers and those more intense ones to *E* isomers of **1** and **2** (Fig. 1).

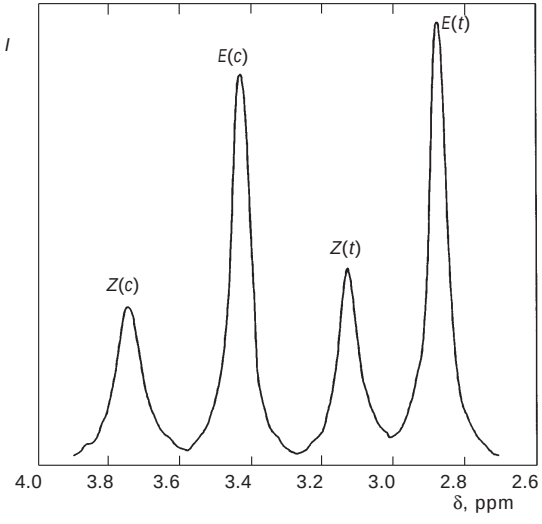

FIG. 1
^{1}H NMR signal of nitrogen-bonded methyl groups in amide 2; L/S = 0.05, *T* = 350 K

NMR Spectra

For the structure determinations and signal assignments, ^1H, ^{13}C and 2D heterocorrelated NMR spectra were measured at 500 MHz on a Bruker Avance DRX-500 spectrometer in chloroform-d_1 (c = 0.1 mol dm^{-3}) with tetramethylsilane as an internal standard. For ^1H NMR kinetic measurements, 0.05 mol dm^{-3} solutions of compound **1** in hexachlorobutadiene with 6 vol.% cyclosilane-d_{18}, $(CH_2Si(CD_3)_2)_3$, (internal standard and ^2H-lock substance), and 0.136 mol dm^{-3} solutions of compound **2** in hexachlorobutadiene with 10.7 vol.% benzene-d_6 (^2H-lock substance) and tetramethylsilane (internal standard) were used; the auxiliary reagent–substrate ratio (L/S) being 0–0.3. ^1H NMR kinetic measurements of amide **2** and determination of the rate constant at coalescence temperature of amide **1** (L/S = 0.1), k_c, were performed at 80 MHz on Bruker WP 80 and Tesla BS 587 NMR spectrometers. The temperature in the NMR probe set with precission of ±0.2 K was checked using the procedure described in refs[2,13,14].

Computer Calculations

The calculations of the rate constant of the interconversion from kinetically broadened signals of compound **2** were carried out on a PC computer using three programs written in our laboratory, whereas, the rate constant of the rotation in amide **1** was calculated using the best program (Simseb) only. The programs were written in programming language Matlab+; their optimization procedure uses a supermodified simplex algorithm[15] which contains a second-order type of vertex with an expansion factor g restricted to be out of the interval 0 ± 0.1 and 1 ± 0.1 to minimize the standard deviation between simulated and experimental spectrum. The programs show an agreement of experimental with theoretical spectrum after each optimization step; the calculation of theoretical line shapes is based on the modified Bloch equations[16].

The program called Simtex, described in ref.[2], has been modified for two doublets with unequally populated sites. Its other versions, Simbex and Simseb, have been developed in order to minimize the number of optimized parameters.

RESULTS AND DISCUSSION

Rate Constant at the Coalescence Temperature

Addition of the shift reagent, Eu(fod)$_3$, to the amide **1** causes shifting of all the signals to the lower field and increasing of the resonance frequency difference of exchanging nuclei. The increase in the rate of rotamer interconversion with increasing temperature causes a decrease in the difference between corresponding signals, $\Delta\nu$, accompanied with their broaden-

+ Matlab is a commercial product of The MathWorks Inc. Natick, U.S.A. supplied by Humusoft s.r.o. Prague. Listing of the Simseb program is available from the authors on request.

ing and finally coalescence to one signal. Since the chemical shift difference between signals, $\Delta\nu$, depends on the magnetic field used, the coalescence can be achieved on the 80 MHz spectrometer at a lower temperature (408 K) than on the 500 MHz one; for this measurement, a pair of nitrogen-bound methyl signals in *trans* position towards carbonyl group was used. As $\Delta\nu$ depends on temperature, the value $\Delta\nu_c$ (difference in chemical shift at the coalescence) must be extrapolated from the kinetically unaffected part of a plot of $\Delta\nu$ *vs* $1/T$ to the coalescence temperature[1]. The total rate constant at coalescence, k_c, was calculated[17] iteratively with Microsof Excel according to Eqs (*1*) and (*2*)

$$4\pi^2 (\nu_1 - \nu)(\nu_2 - \nu)(2\nu - \nu_1 - \nu_2) + k_c^2 (\nu - p_1\nu_1 - p_2\nu_2) = 0 \qquad (1)$$

$$4\pi^2 \left[(\nu_1 - \nu)(\nu_2 - \nu) + (2\nu - \nu_1 - \nu_2)^2\right] + k_c^2 = 0 \quad , \qquad (2)$$

where the used symbols have the same meaning as in ref.[1]. The k_c found is equal to 19.7 s^{-1}.

Rate Constant from the Line Shape Analysis

For the determination of the rate constant of rotation in a temperature interval below coalescence (350–382 K for **2** or 380–415 K for **1**), the change in the shape of two pairs of nitrogen-bound methyl signals was analyzed by the line shape analysis (Fig. 1). The rate constant for a single intramolecular process was determined by analysis of signal shapes corresponding to two different molecular groups, which makes it possible to get more reliable results. The spectra were measured for the reagent–substrate ratios (L/S) from 0 to 0.3. This procedure aimed to prove that the presence of an auxiliary compound does not affect the experimental rate of rotation. The NMR spectra of the pairs of signals were digitalized into two vectors: vector of chemical shifts in Hz, ν, and vector of corresponding amplitudes, $\boldsymbol{I}_{exp}$. For each chemical shift in the selected range, ν, theoretical amplitude $\boldsymbol{I}_{calc}$ was calculated[18] according to Eqs (*3*) and (*4*):

$$\boldsymbol{K} \cdot \boldsymbol{G} = \mathrm{i}\, \boldsymbol{C} \cdot \boldsymbol{P} \qquad (3)$$

$$\mathbf{K} = 2\pi\mathrm{i}\begin{bmatrix} \nu_1 & 0 & 0 & 0 \\ 0 & \nu_2 & 0 & 0 \\ 0 & 0 & \nu_3 & 0 \\ 0 & 0 & 0 & \nu_4 \end{bmatrix} - 2\pi\mathrm{i}\begin{bmatrix} \nu & 0 & 0 & 0 \\ 0 & \nu & 0 & 0 \\ 0 & 0 & \nu & 0 \\ 0 & 0 & 0 & \nu \end{bmatrix} + \\ + \pi\begin{bmatrix} b_1 & 0 & 0 & 0 \\ 0 & b_2 & 0 & 0 \\ 0 & 0 & b_3 & 0 \\ 0 & 0 & 0 & b_4 \end{bmatrix} - k\begin{bmatrix} -1 & +1 & 0 & 0 \\ +1 & -1 & 0 & 0 \\ 0 & 0 & -1 & +1 \\ 0 & 0 & +1 & -1 \end{bmatrix}, \qquad (4)$$

where the used symbols have the same meaning as in ref.[2], except for the fractional population vector, $\boldsymbol{P} = (p_1, p_2, p_1, p_2)'$, containing four elements.

Experimental and theoretical spectra (*i.e.*, vectors $\boldsymbol{I}_{\mathrm{exp}}$ and $\boldsymbol{I}_{\mathrm{calc}}$) were then normalized and compared with the help of standard deviation of their difference. Afterwards, the first estimates of the parameters in Eqs (*3*) and (*4*) were changed according to the super-modified Simplex algorithm[15] until the calculated spectrum fitted the experimental one with a defined precision. The first estimate of chemical shifts was obtained by extrapolating the linear part of a plot of the $\Delta\nu$ *vs* $1/T$; the estimated line widths were taken from the spectral lines at lower temperature. The determination of the rate constant from each spectrum was divided into two steps. In the first step, the iterative procedure only involved a variation of the rate constant (the program was adapted from ref.[16]). Its optimum value was taken as a starting estimate for the next step which was performed using three different programs.

In the Simtex program, the optimization procedure includes ten spectral parameters: four chemical shifts, ν_1–ν_4, four line widths without exchange broadening, b_1–b_4, the total rate constant, k, and an isomer ratio, $p = p_1/p_2$. The total rate constant is the sum of the individual rate constants for the forward and reverse transitions between isomers Z and E, $k_1(Z \rightarrow E)$ and $k_2(E \rightarrow Z)$. The individual rate constants can be calculated from the total value using Eqs (*5*) and (*6*).

$$k_1 = k\, p_2 \qquad (5)$$

$$k_2 = k\, p_1 \qquad (6)$$

In the Simbex program, nine optimization parameters were used since four line widths, $\boldsymbol{b}$, were replaced by three optimized parameters, $\boldsymbol{u} = (u_1, u_2, u_3)$, defined in Eq. (*7*)

$$= u_1 + u_2 \quad + u_3 \quad , \tag{7}$$

where $\boldsymbol{P}$ is a fractional population vector (from Eq. (*3*)) and $\boldsymbol{L}$ an induced chemical shift vector which expresses an influence of a shift reagent on line widths of the corresponding four NMR lines.

The Simseb program uses six spectral parameters optimized alternatively in blocks of fifty simplex steps: always two chemical shifts and two line widths corresponding to one pair of signals were set constant and those from another pair of signals were optimized together with *k* and *p*. Then these optimized parameters were set constant and the others, previously constant, were optimized, *etc*.

For comparison of the programs used for the determination of the rate constant of rotation for amide **2**, the same criteria as in ref.[2] were used but with necessary modifications due to the number of optimized parameters. The standard estimate and the confidence interval of the rate constants were obtained from the spectrum measured at 360 K; when using other criteria, all measurements were included.

For determination of the confidence interval of the rate constant, the optimum values were increased (+) or decreased (–) in their twelve combinations, instead of eight combinations as in ref.[2], because the number of spectral parameters is ten instead of five, according to the Plackett–Burman reduced factorial experiment[19,20] (Table I). The population ratio was varied within about 2 per cent. The results of testing are summarized in Table II.

In the Simtex program, the number of the optimized parameters has turned out to be too large for finding their optimum values. In the Simbex program, reduction of one in the number of the parameters has not much improved the optimum values. Our third program Simseb gives the smallest standard deviation between calculated and experimental spectra, the best coefficient of determination for Arrhenius equation, the narrowest average error range of the rate constants and the smallest confidence interval of the rate constants. Summarizing, we believe that the rate constants determined by the Simseb program can be considered the best values. The values given in Tables III and IV are the total rate constants of isomerization ($k = k_1 + k_2$) calculated by the Simseb program.

TABLE I
Trials according to the Plackett–Burman[19] reduced factorial experiment[a]

Parameter	ν_1[b,e]	ν_2[b,e]	ν_3[b,e]	ν_4[b,e]	Dummy	b_1[b,e]	b_2[b,e]	b_3[b,e]	b_4[b,e]	k[c,f]	p[d]
Input	40.4	68.8	101.8	119.2		3.85	2.50	2.77	1.96	8.24	0.586
1	+	+	–	+	+	+	–	–	–	+	–
2	+	–	+	+	+	–	–	–	+	–	+
3	–	+	+	+	–	–	–	+	–	+	+
4	+	+	+	–	–	–	+	–	+	+	–
5	+	+	–	–	–	+	–	+	+	–	+
6	+	–	–	–	+	–	+	+	–	+	+
7	–	–	–	+	–	+	+	–	+	+	+
8	–	–	+	–	+	+	–	+	+	+	–
9	–	+	–	+	+	–	+	+	+	–	–
10	+	–	+	+	–	+	+	+	–	–	–
11	–	+	+	–	+	+	+	–	–	–	+
12	–	–	–	–	–	–	–	–	–	–	–

[a] For the parameters of the NMR spectrum of 2 measured at 360 K and L/S = 0.1, optimized by the Simseb program. [b] Varied ±0.5 Hz from the input values. [c] Varied ±20% from the input value. [d] Varied ±2% from the input value. [e] In Hz. [f] In s^{-1}.

TABLE II
Criteria[a] for comparison of optimization program at L/S 0.1 and 0.2

Criterion	Simseb		Simtex		Simbex	
	0.1	0.2	0.1	0.2	0.1	0.2
Standard deviation · 10^2	1.538	1.554	1.660	1.687	1.741	1.763
Coefficient of determination	0.9998	0.9996	0.9977	0.9987	0.9933	0.9985
Average error range, s^{-1}	0.215	0.223	0.288	0.294	0.252	0.268
Confidence interval of the rate constant, s^{-1}	0.240	0.237	0.245	0.253	0.296	0.274

[a] For definitions, see ref.[2]

Values of the rate constants in Fig. 2 determined by NMR spectroscopy fit perfectly the linear dependence of logarithms of the individual rate constants on reciprocal temperature (see coefficient of determination in Table II) for both studied compounds. Arrhenius plots for amide **1** show a good agreement between the results obtained by line shape analysis and at the coalescence temperature. The results in the Tables III and IV showing the total rate constants can be considered independent of an amount of the shift reagent which makes it possible to use the rate constant values obtained at all reagent–substrate ratios for the evaluation of a single Arrhenius equation. For instance, parameters a_1 and a_2 for a single reagent–substrate

TABLE III
Total rate constants of isomerization (s^{-1}) of **2** from line shape analysis at different temperatures T (K)

L/S	350	360	370	373	375	378	380	382
0.05	3.53	8.37	17.9	23.2	26.1			
0.10	3.63	8.23	18.5		26.4	33.3		
0.15	3.56	8.28	18.4		26.2		38.8	43.8
0.20	3.61	8.17	18.5				37.7	
0.30		8.37	17.9		26.7		38.1	

TABLE IV
Total rate constants of isomerization (s^{-1}) of **1** fromline shape analysis and coalescence at different temperatures T (K)

L/S	380	385	390	395	400	405	408	410	415
0.00	2.32	3.49	5.08	7.48	10.6	15.6			
0.05			5.17	7.35	10.9	15.3		21.9	30.4
0.10			5.06	7.51	10.6	15.5	19.7[a]	21.8	31.0
0.15			5.11	7.32	10.9	15.2		22.0	30.4
0.20			5.01	7.49	10.7	15.7		21.4	30.7
0.25			5.19	7.29	10.9	15.2		22.0	30.2
0.30			5.02	7.56	10.7	15.6		21.8	30.9

[a] From coalescence at 80 MHz.

ratio, L/S = 0.1 (n = 5) and parameters obtained from regression including all individual rate constants, k_1 (n = 24) for substance **2** agree very well; *cf.* Eqs (*8*) and (*9*).

$$n = 5\,, \quad \ln y = -10\,396_{(\pm 139)}\, x + 30.54_{(\pm 0.37)} \tag{8}$$

$$n = 24\,, \quad \ln y = -10\,339_{(\pm 66)}\, x + 30.38_{(\pm 0.18)} \tag{9}$$

Values in parentheses in Eqs (*8*) and (*9*) are standard deviations of the corresponding parameters; it is clear that an increased precision has been achieved due to inclusion of larger number of measurements.

Determination of Activation Parameters

The activation energies, E_a, for forward and reverse isomerizations were determined according to exponential Arrhenius equation as in ref.[2] and the enthalpy and entropy of activation[21], $\Delta H^{\neq}$ and $\Delta S^{\neq}$, were calculated using Eqs (*10*) and (*11*) from ref.[2]. Then the Gibbs energy of activation[21], $\Delta G^{\neq}$, was calculated as $\Delta G^{\neq} = \Delta H^{\neq} - T\Delta S^{\neq}$ at the harmonic average of temperatures for

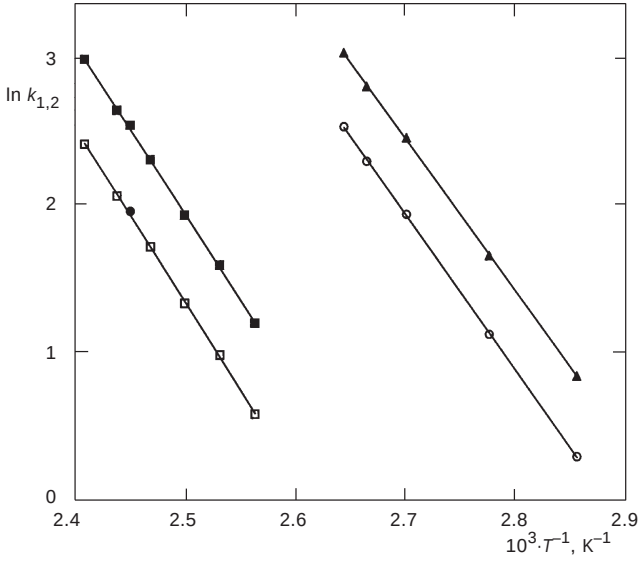

FIG. 2
Arrhenius plot of individual rate constants for L/S = 0.1; line shape analysis by the Simseb program (subscript 1 for $Z \rightarrow E$, subscript 2 for $E \rightarrow Z$ isomerization): ▲ k_1 (**2**), ❍ k_2 (**2**), ■ k_1 (**1**), ❒ k_2 (**1**), ● coalescence

the NMR measurements with the line shape analysis, 402.3 K (**1**) or 367.3 K (**2**). For the error determination of activation parameters, $\Delta\Delta H^{\neq}$, $\Delta\Delta S^{\neq}$ and $\Delta\Delta G^{\neq}$, Eqs (12)–(14) from ref.[2] were used. The error in the temperature measurement, ΔT, was taken equal to ±0.5 K (for reasoning, see ref.[2]) and the error in the rate constant, Δk, was estimated to be equal to the average error range in Table II.

Activation parameters obtained for each L/S ratio independently are collected in Table V. Those calculated for all concentrations of the auxiliary reagent (Table VI) give much lower error values. This fact is especially important in the case of entropy terms; the results in Table V do not make possible to find the sign of this thermodynamic parameter due to high error values in its determination. On the other hand, the corresponding values in Table VI are loaded by relatively small errors showing definitely negative

TABLE V
Activation parameters[a] at 402.3 K (**1**) and 367.3 K (**2**)

L/S	$\Delta H_1^{\neq b}$	$\Delta S_1^{\neq c}$	$\Delta G_1^{\neq b}$	$\Delta H_2^{\neq b}$	$\Delta S_2^{\neq c}$	$\Delta G_2^{\neq b}$
			Compound **1**			
0.00	93.6 ± 0.1	2.7 ± 3.3	92.5 ± 1.5	95.6 ± 0.2	2.8 ± 3.5	94.5 ± 1.6
0.05	91.6 ± 0.1	–2.3 ± 3.2	92.5 ± 1.4	93.5 ± 0.2	–2.5 ± 3.4	94.5 ± 1.5
0.10	93.6 ± 0.1	2.6 ± 3.3	92.5 ± 1.5	95.5 ± 0.2	2.5 ± 3.5	94.5 ± 1.6
0.15	92.0 ± 0.1	–1.3 ± 3.2	92.5 ± 1.5	93.9 ± 0.2	–1.4 ± 3.4	94.5 ± 1.6
0.20	92.3 ± 0.1	–0.5 ± 3.3	92.5 ± 1.5	94.3 ± 0.2	–0.6 ± 3.4	94.5 ± 1.6
0.25	90.0 ± 0.1	–3.9 ± 3.2	92.5 ± 1.4	92.8 ± 0.2	–4.1 ± 3.4	94.5 ± 1.5
0.30	92.9 ± 0.1	1.0 ± 3.3	92.5 ± 1.5	94.9 ± 0.2	0.9 ± 3.5	94.5 ± 1.6
			Compound **2**			
0.05	83.1 ± 0.2	–2.0 ± 2.2	83.8 ± 1.0	84.6 ± 0.2	–2.2 ± 2.2	85.4 ± 1.0
0.10	83.4 ± 0.2	–1.1 ± 2.2	83.8 ± 1.0	85.0 ± 0.2	–1.0 ± 2.2	85.4 ± 1.0
0.15	83.0 ± 0.2	–2.2 ± 2.2	83.8 ± 1.0	84.6 ± 0.2	–2.0 ± 2.2	85.4 ± 1.0
0.20	81.8 ± 0.2	–5.3 ± 2.2	83.8 ± 1.0	83.4 ± 0.2	–5.4 ± 2.2	85.4 ± 1.0
0.30	83.2 ± 0.2	–1.6 ± 2.2	83.8 ± 1.0	84.7 ± 0.2	–1.9 ± 2.2	85.4 ± 1.0

[a] Subscript 1 for $Z \rightarrow E$, subscript 2 for $E \rightarrow Z$ isomerization; errors calculated using Eqs (*12*)–(*14*) from ref.[2] [b] In kJ mol^{-1}. [c] In J K^{-1} mol^{-1}.

values of entropy terms in Simseb calculations. As the Simseb program gives the smallest errors, its preference over Simtex and Simbex is obvious.

Determination of Standard Isomerization Parameters

The standard enthalpy and entropy of isomerization, ΔH^0 and ΔS^0, were calculated according to Eq. (*10*); the used values of the isomer population ratio are shown in Tables VII and VIII.

$$\ln p = -\frac{\Delta H^0}{R}\frac{1}{T} + \frac{\Delta S^0}{R} + \varepsilon \qquad (10)$$

The isomer population ratio, p, expresses the equilibrium constant, K. For evaluation of the energy difference between isomers Z and E, standard Gibbs energy of isomerization, ΔG^0, was calculated from standard enthalpy and entropy of isomerization, $\Delta G^0 = \Delta H^0 - T\Delta S^0$, at the harmonic average of

TABLE VI
Comparison of activation parameters of isomerization[a] at 402.3 K (**1**) and 367.3 K (**2**)

Activation parameters	Simseb		Simtex	Simbex
	1	**2**	**2**	**2**
$\Delta H_1^{\neq b}$	92.2	82.9	85.7	87.6
$\Delta\Delta H_1^{\neq b}$	0.1	0.2	0.2	0.1
$\Delta S_1^{\neq c}$	–0.7	–2.4	5.6	10.3
$\Delta\Delta S_1^{\neq c}$	0.4	0.5	0.5	0.4
$\Delta G_1^{\neq b}$	92.5	83.8	83.6	83.8
$\Delta\Delta G_1^{\neq b}$	0.3	0.3	0.3	0.3
$\Delta H_2^{\neq b}$	94.2	84.5	87.3	89.1
$\Delta\Delta H_2^{\neq b}$	0.2	0.2	0.2	0.2
$\Delta S_2^{\neq c}$	–0.8	–2.4	5.6	10.3
$\Delta\Delta S_2^{\neq c}$	0.5	0.4	0.4	0.5
$\Delta G_2^{\neq b}$	94.5	85.4	85.2	85.4
$\Delta\Delta G_2^{\neq b}$	0.4	0.3	0.3	0.3

[a] Calculated from k values at all L/S rations. [b] In kJ mol^{-1}. [c] In J K^{-1} mol^{-1}.

temperatures for the NMR measurements with the line shape analysis of 402.3 K (**1**) and 367.3 K (**2**). For the error determination of standard thermodynamic parameters of isomerization, $\Delta\Delta S^0$, $\Delta\Delta H^0$ and $\Delta\Delta G^0$, Eqs (*11*)–(*13*) were used.

$$\Delta\Delta S^0 = \frac{\partial \Delta S^0}{\partial T}\Delta T + \frac{\partial \Delta S^0}{\partial K}\Delta K = -\frac{\Delta H^0}{T^2}\Delta T + \frac{R}{K}\Delta K \qquad (11)$$

$$\Delta\Delta H^0 = (-R \ln K + \Delta S^0)\,\Delta T - \frac{RT}{K}\Delta K \qquad (12)$$

$$\Delta\Delta G^0 = \Delta\Delta H^0 + T\,\Delta\Delta S^0 \qquad (13)$$

TABLE VII
Population ratios p of **2** after optimization at different temperatures T (K)

L/S	350	360	370	373	375	378	380	382
0.05	0.577	0.586	0.595	0.596	0.599			
0.10	0.578	0.586	0.594		0.599	0.601		
0.15	0.577	0.586	0.594		0.599		0.603	0.605
0.20	0.576	0.586	0.594				0.602	
0.30		0.586	0.594		0.599		0.602	

TABLE VIII
Population ratios p of **1** after optimization at different temperatures T (K)

L/S	380	385	390	395	400	405	408	410	415
0.00	0.530	0.535	0.540	0.544	0.548	0.552			
0.05			0.540	0.544	0.548	0.551		0.556	0.560
0.10			0.540	0.544	0.548	0.552	0.554[a]	0.556	0.560
0.15			0.540	0.543	0.548	0.552		0.556	0.560
0.20			0.540	0.544	0.548	0.552		0.556	0.560
0.25			0.540	0.543	0.548	0.552		0.556	0.560
0.30			0.539	0.544	0.548	0.553		0.556	0.560

[a] From coalescence at 80 MHz.

TABLE IX
Energy difference between isomers *E* and *Z* at 402.3 K (**1**) and 367.3 K (**2**)

L/S	ΔH^{0a}	ΔS^{0b}	ΔG^{0a}	$\Delta G^{0a,c}$
		Compound **1**		
0.00	2 040 ± 28	0.10 ± 0.07	1 999 ± 56	1 998
0.05	1 969 ± 28	–0.08 ± 0.07	2 001 ± 56	1 997
0.10	1 966 ± 28	–0.08 ± 0.07	1 999 ± 56	2 001
0.15	1 962 ± 28	–0.09 ± 0.07	2 000 ± 56	1 996
0.20	1 971 ± 28	–0.07 ± 0.07	2 001 ± 56	1 995
0.25	1 956 ± 28	–0.11 ± 0.07	2 000 ± 56	2 001
0.30	1 997 ± 28	–0.01 ± 0.07	2 000 ± 56	2 001
		Compound **2**		
0.05	1 574 ± 24	–0.07 ± 0.06	1 600 ± 47	1 604
0.10	1 584 ± 24	–0.04 ± 0.04	1 598 ± 47	1 595
0.15	1 600 ± 24	0.00 ± 0.06	1 599 ± 47	1 609
0.20	1 603 ± 24	0.01 ± 0.06	1 601 ± 47	1 605
0.30	1 562 ± 24	–0.10 ± 0.06	1 600 ± 47	1 605

[a] In J mol^{-1}. [b] In J K^{-1} mol^{-1}. [c] Calculated from $\Delta G_2^{\neq} - \Delta G_1^{\neq}$

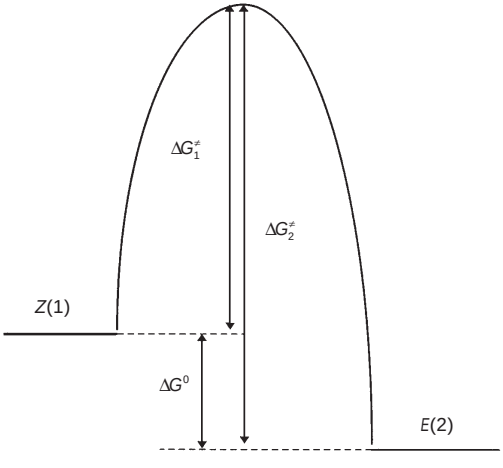

FIG. 3
Comparison of Gibbs energy of activation, $\Delta G^{\neq}$, and standard Gibbs energy of isomerization, ΔG^0

The error in the temperature measurement, ΔT, was taken equal to ±0.5 K and the error in the isomer ratio, $p \equiv K$, was estimated as 0.005.

The calculated standard thermodynamical parameters of isomerization (Table IX) show that the standard Gibbs energy of isomerization is independent of the reagent–substrate ratio, L/S, for both studied amides **1** and 2.

A relation between the Gibbs energy of activation, $\Delta G^{\neq}$, and the standard Gibbs energy of isomerization, ΔG^0, is demonstrated in Fig. 3.

Comparison of the standard Gibbs energy of isomerization with the values obtained as differences between the Gibbs energies of activation for reverse and forward transitions, $\Delta G^0 = \Delta G_2^{\neq} - \Delta G_1^{\neq}$, shows that both values lie in a confidence interval.

The Gibbs energy of activation for both transitions of amide **1** was found by 9.0 and 8.6 kJ mol^{-1} higher than those of amide **2** at 402.3 K. This result is in accordance with our expectation that a more bulky substituent leads to an increase of the rotation barrier. It also supports our anticipation about the *E–Z* isomerization *via* the keto group rotation since for amide group rotation only negligible effect of the distant substituent could be expected.

Conclusion

In order to get precise values of the rate constant of isomerization from the line shape analysis, it is useful to analyze two independent pairs of signals. From the three optimization programs, the Simseb program was found the best one. The problem of a large number of optimized parameters was solved in this program using a modified optimization procedure consisting in optimizing six parameters corresponding to one pair of signals alternatively in blocks of fifty simplex steps. If the rate constant values are independent on the amount of the shift reagent, those obtained at all reagent–substrate ratios can be used for an Arrhenius plot, which results in more reliable thermodynamic parameters. Advantages of a non-linear regression for the calculation of activation parameters from Arrhenius equation were discussed in ref.[2]. The standard Gibbs energy of isomerization and the values obtained as differences between the Gibbs energies of activation for reverse and forward transitions lie in the confidence interval, thus showing that indepedently determined rate constants and isomer ratios are quite accurate. Combining precise measurements of experimental variables (including temperature) and analyzing two independent pairs of signals with a suitable optimization algorithm and non-linear regression results in an increased accuracy of the calculated rate constants and thermodynamic parameters for the exchange between two unequally populated sites.

We would like to thank Dr M. Nechvátal, Lachema Brno, for his help with the sample preparations.

REFERENCES

1. Holík M., Mannschreck A.: *Org. Magn. Reson.* **1979**, *12*, 28.
2. Přibylová E., Holík M.: *Collect. Czech. Chem. Commun.* **1998**, *63*, 955.
3. Cuyegkeng M. A., Mannschreck A.: *Chem. Ber.* **1987**, *120*, 803.
4. Holík M., Mannschreck A.: *Org. Magn. Reson.* **1979**, *12*, 223.
5. Küspert R., Mannschreck A.: *Org. Magn. Reson.* **1982**, *19*, 6.
6. Mannschreck A., Jonas V., Kolb B.: *Angew. Chem.* **1973**, *85*, 590, 994.
7. Lefevre T., Burgemeister T., Mannschreck A.: *Tetrahedron Lett.* **1977**, 1125.
8. Klabuhn B., Clausen E., Goetz H.: *Tetrahedron* **1973**, *29*, 1153.
9. Holík M., Skála V., Čiernik J.: *Chem. Zvesti* **1975**, *29*, 533.
10. Holík M., Mistr A., Láznička V.: *Collect. Czech. Chem. Commun.* **1978**, *43*, 739.
11. Solčániová E., Hrnčiar P., Liptaj T.: *Org. Magn. Reson.* **1982**, *18*, 55.
12. Steinmetz W. E.: *J. Am. Chem. Soc.* **1973**, *95*, 2777.
13. Cavanagh J.: *Protein NMR Spectroscopy: Principles and Practice*, p. 168. Academic Press, New York 1996.
14. Friebolin H., Schilling G., Pohl L.: *Org. Magn. Reson.* **1979**, *12*, 569.
15. Morgan E., Burton K. W.: *Chemom. Intell. Lab. Syst.* **1990**, *8*, 97.
16. Martin M. L., Delpuech J.-J., Martin G. J.: *Practical NMR Spectroscopy*, p. 441. Hayden & Son, London 1980.
17. Shanan-Atidi H., Bar-Eli K. H.: *J. Phys. Chem.* **1970**, *74*, 961.
18. Sandström J.: *Dynamic NMR Spectroscopy*, p. 13. Academic Press, London 1982.
19. Plackett R. L., Burman J. P.: *Biometrika* **1946**, *33*, 305.
20. Jones K.: *Int. Lab.* **1986**, *16*, 32.
21. Reeves L. W., Shaw K. N.: *Can. J. Chem.* **1971**, *49*, 3671.